

## ORIGINAL ARTICLE

# Synthesis and Characterization of Chitosan-Silver Nanocomposite Using Chemical Reduction Method and their Antibacterial Properties

Ansab Ali Zaidi<sup>a</sup>, RY Khosa<sup>a</sup>, A. Atiq<sup>a</sup>, M. Usman<sup>a</sup>, Imosobomeh L. Ikhioya<sup>b,c,\*</sup>

<sup>a</sup>Department of Physics, University of Education Lahore, DG Khan Campus 32200, Pakistan

<sup>b</sup>Department of Physics and Astronomy, University of Nigeria Nsukka, 410001, Nigeria

<sup>c</sup>National Centre for Physics, Quaid-i-Azam University Campus, Islamabad, 44000, Pakistan

## KEYWORDS

chitosan, silver,  
nanoparticles,  
FTIR,  
antibacterial

## ABSTRACT

This study synthesized chitosan silver nanocomposite using chemical reduction and ultraviolet irradiation. This method is straightforward and yields abundant products in brief intervals of time. The targeted composite is got without using toxic chemical reagents which might contribute to antibacterial, antifungal, and anticancer activities. Chitosan silver nanocomposites got in this method have a large surface-to-volume ratio. The presence of chitosan silver nanocomposite in the prepared sample is confirmed by an ultraviolet-visible (UV-VIS) spectrophotometer, a typical plasmonic peak for silver nanoparticles was observed at 440 nm. The structural and functional groups induced in the product sample due to the presence of chitosan silver nanocomposites are confirmed by FTIR. The antimicrobial application against gram-positive and gram-negative bacteria is confirmed by the zone of inhibition created by nanocomposites. This study could provide a basic understanding to prepare polymeric-metal composites for antibacterial applications.

## ARTICLE HISTORY

Received: June 17, 2023

Revised: August 27, 2023

Accepted: October 01, 2023

Published: October 03, 2023

## 1 Introduction

Metal nanoparticles offer a promising option to combat antibiotic resistance due to their unique activity systems and are widely used by researchers. Their unique systems fight harmful microbes and target biomolecules that prevent safe strains from growing [1]. Among different nanomaterials, valuable metal nanomaterials stand out such as (silver, gold, copper, iron, zinc, platinum, and so on) due to their magnificent optical, electronic, and reactant properties [2].

Metal nanoparticles such as silver have attractive physicochemical characteristics, making them important in science. Silver nanoparticles (AgNPs) have antifungal, anti-inflammatory, antiviral, antibacterial, antiangiogenic, and antiplatelet effects.

In various investigations [2] – [4], metallic nanoparticles' antibacterial properties can be increased by combining them with chitosan, a natural biopolymer. Their unique characteristics make them useful for a variety of purposes, including being used as antibacterial agents, in industrial, domestic, and healthcare-related products, and in consumer goods, medical device coatings, optical sensors, cosmetics, pharmaceuticals, and food. They are also used in diagnostics, orthopedics, drug delivery, as anticancer agents, and to improve the effectiveness of anticancer medications on tumors [5].

Through the stability and support of nanoparticles, several AgNPs-based composites have shown improved performance. Chitosan-Silver Nanoparticles (CS/AgNPs) nanocomposites are a type of bio-nanostructured hybrid material, due to their biocompatibility and biodegradability. CS is considered a non-toxic biopolymer, besides having superior antibacterial and

\* CORRESPONDING AUTHOR | I. L. Ikhioya, ✉ [imosobomeh.ikhioya@unn.edu.ng](mailto:imosobomeh.ikhioya@unn.edu.ng)

antifungal activity compared to other polymers and biopolymers [6].

There are many ways to make Ag-Chitosan nanocomposites, including the in-situ reduction approach [3], electrochemical deposition [4], [5], [6], microwave-assisted method [7], [8], chemical reduction method [9], [10], and bio-synthesis methods [11], etc. Among all the methods for synthesis, chemical reduction is the most preferred.

Chemical reduction is among the top techniques used in research labs to create nanoparticles [12]. The chemical reduction process consists of three crucial steps. The metallic salts are reduced using reducing agents, while the particle size is controlled by a capping agent and the ionic complexes are stabilized. The antibacterial action of Nanocomposites containing Chitosan Silver is against gram-positive and gram-negative bacteria. The ability to adapt is crucial for combating germs and avoiding drug resistance.

The growth of several harmful bacteria, such as *E. coli*, *S. aureus*, and *P. aeruginosa*, can be prevented by chitosan and silver nanoparticles. Chitosan-silver nanocomposites can be excellently produced using the chemical reduction method. The combination of chitosan and silver nanoparticles in nanocomposites enhances their antibacterial properties. By altering particles size, shape, and composition, one can optimize and personalize. Chitosan-silver nanocomposites are useful for medical, food, and water applications due to their antibacterial properties.

In the current study, the chemical reduction approach is used to synthesize silver-chitosan nanocomposite. We used a UV-visible spectrophotometer and two spectroscopies to examine the silver nanocomposite.

## 2 Experimental Section

### 2.1 Materials

Chitosan with an 85% deacetylation is got from Sigma Aldrich. The solution of dimethyl sulfoxide (DMSO) was gotten from the local university laboratory. Silver nitrate ( $\text{AgNO}_3$ ) and Tris ( $(\text{HOCH}_2)_3\text{CNH}_2$ ) are bought from Sigma Aldrich.

### 2.2 Preparation of Stock Solutions

The chitosan silver composite is made with a simple and inexpensive chemical reduction method. First, we have formed the stock solution of 5 mg chitosan dissolved in 1 ml of Dimethyl sulfoxide (DMSO). Similarly, we have prepared a 20 mM stock solution of  $\text{AgNO}_3$  in Milli-Q water. We made a 20 mM stock solution of Tris in milli Q-water which is used to maintain the pH of the solution at about a value of 7.4.

We prepared a sample solution by taking 50  $\mu\text{l}$  volume from a stock solution of  $\text{AgNO}_3$  with the help of a pipette. Similarly, 50  $\mu\text{l}$  chitosan solution is taken from the stock solution and mixed with  $\text{AgNO}_3$  by using the pipet. Now the sample contains 50  $\mu\text{l}$   $\text{AgNO}_3$  and 50  $\mu\text{l}$  chitosan in D-vials.

To maintain the pH of the solution we added the buffer solution of 200  $\mu\text{l}$  and 700  $\mu\text{l}$  of Milli-Q water in the sample. The sample is stirred for 10 to 20 minutes continuously at room temperature for uniform dispersion. The total volume of the sample becomes 1 ml. The color of the sample is milky white.

### 2.3 Reduction Process

We placed the sample in the chamber of a UV lamp for irradiation for reduction in the presence of UV light. The sample changes to dark brown after 10 minutes of irradiation at 254 nm, showing the reduction and preparation of chitosan silver nanocomposite.

### 2.4 Characterizations

XRD, UV-visible spectroscopy and FTIR are used to characterize the chitosan silver nanocomposite sample. Antibacterial testing was conducted on the prepared sample.

## 3 Results and Discussions

### 3.1 UV-visible Spectroscopy

Figure 1(a) displays the absorption spectra chitosan NPs, (b) Ag-Ch composite which can be detected using the straightforward and highly sensitive technique of UV-Visible spectroscopy. UV-Visible spectroscopy is a crucial method for verifying the formation and stability of metal nanoparticles in a solution, based on the optical phenomenon of LSPR [13].

The absorption spectra presented in Figure 1(a) demonstrate an absorption peak of around 252 nm. According to [14], this peak is observed due to the  $\pi$ - $\pi^*$  transition of the chitosan nanoparticles, whereas Figure 1(b) shows that Ag-chitosan nanocomposite exhibit an absorption band with a peak centered at 440 nm, which is known as a localized surface plasmon resonance (LSPR) [15].

Furthermore, the exhibited absorption band around 440 nm suggested the reduction of Ag by chitosan [16]. LSPR (localized surface plasmon resonance) is distinct from SPR (surface plasmon resonance) because LSPR involves the localized oscillation of electrons induced within nanostructures, rather than along the surface of the metal-dielectric.

Additionally, the width of the observed absorption band is narrower, which can be attributed to the medium molecular weight of chitosan. This factor is known to act as both a nucleation controller and stabilizer for the nanoparticles [17]. In addition, the observed absorption band at 440 nm indicated that Ag was being reduced by chitosan [18]. The 220 nm absorption peak is significant because it offers important details on the electrical makeup and potential uses of chitosan. Chitosan may interact with UV radiation and exhibit photochemical or photophysical properties, according to the reported absorption behavior. This discovery provides opportunities for applications in fields like phototherapy, UV-blocking polymers, and UV-responsive components for sensors and detectors. This absorption peak's existence at a

longer wavelength than chitosan alone suggests that including silver nanoparticles alters the chitosan matrix's optical characteristics.

AgNPs' plasmonic effects may be responsible for the improved light absorption and scattering capabilities that result from their interaction with chitosan. According to this result, the chitosan-Ag nanocomposite may have distinctive optical characteristics that make it suited for uses including photocatalysis, optical sensors, and surface-enhanced Raman spectroscopy (SERS).

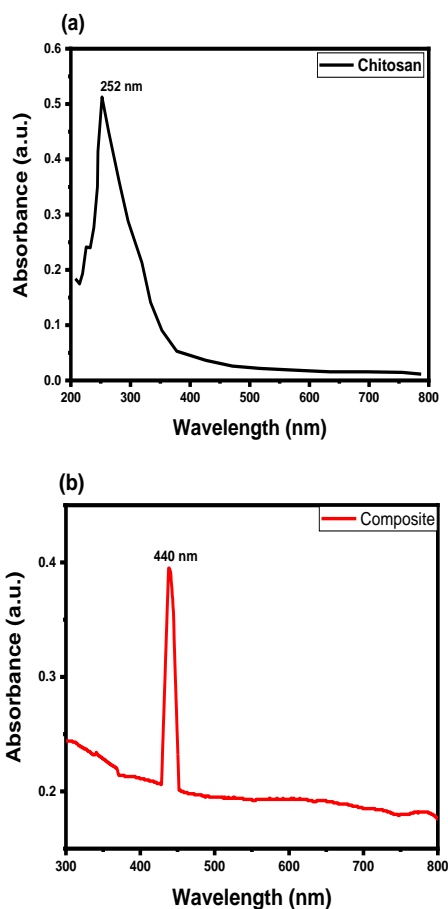


Figure 1: The UV-Visible spectra of (a) chitosan NPs (b) Ag-Ch composite

### 3.2 XRD study of chitosan and silver nanocomposite

Using the XRD technique, the structural characteristics of the produced chitosan and silver nanocomposite were examined. Figure 2 displays the XRD pattern for chitosan and silver nanocomposite that was obtained at 2theta values of (34.951, 43.260, 50.393, and 74.126°), the peaks were visible. The solvent's properties broaden the peaks. The XRD pattern shows no peaks associated with impurities.

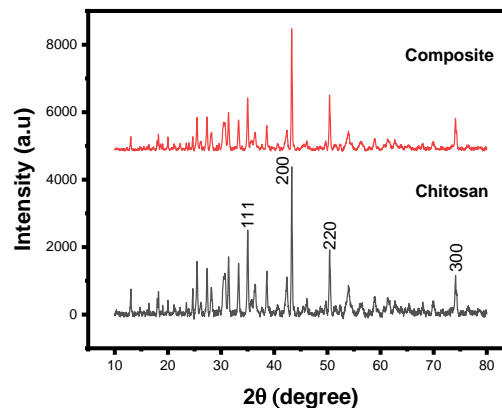


Figure 2: XRD pattern of chitosan and composite

The composite's XRD pattern, which is depicted in Figure 2, shows that silver formed in a single phase and is in perfect accord with the JCPDS card no. 01-089-3897. Peak fitting was performed on the resulting pattern, and the simple cubic crystal structure and lattice parameters were found in Table 1. The pattern contains the  $(hkl)$  values. Table 1 displays the average crystallite size of the chitosan and silver nanocomposite as determined by the Scherrer formula [22] – [24]. The XRD pattern of the chitosan and silver nanocomposite, which is depicted in the pattern, reveals the existence of chitosan as well as silver peaks. This appears to be consistent with the values mentioned in the literature [21].

### 3.3 Fourier Transform Infrared spectroscopy (FTIR)

An FTIR spectral analysis was performed to investigate the molecular interaction between chitosan and silver nanoparticles. Figure 3(a) displays the FTIR spectrum of pure chitosan, with bands indicating N–H and O–H stretching at 3458  $\text{cm}^{-1}$  and  $\text{NH}_2$  bending at 1644  $\text{cm}^{-1}$ .

In Figure 3, the FTIR spectra of chitosan-capped silver nanoparticles display a band of chitosan at wave number 3403  $\text{cm}^{-1}$  representing the amide A band. Amide A is formed primarily as a result of O–H and N–H stretching vibrations. The amide is at 3155  $\text{cm}^{-1}$ , a band of Chi-Ag-NPs is likewise split into a peak. These modifications could be attributed to interactions between chitosan and Ag-NPs' main amino and amide groups [19].

Normally, the O–H and N–H functional groups have a strong affinity for silver ions. Deprotonation sites, which may boost free electron binding to the metal, are critically defined by the difference in electronegativity between the oxygen and nitrogen atoms. Amido is the Hydrogen bonding that is enhanced in Chi-Ag-NPs composites, as seen by a broader band compared to chitosan. The absence of the  $\text{NH}_2$  double spike peak and the presence of the functional groups suggests that the polymer effectively encapsulated the nanoparticles of silver that were created [20].

Table 1: Structural parameters of chitosan and composite

Films	2 $\theta$ (deg.)	$\Delta$ (Å)	( $\Delta$ )	( $\beta$ )	( $hkl$ )	(D) nm	$\sigma$ lines/m <sup>2</sup> $\times 10^{13}$
Chitosan	34.951	2.564	4.442	0.0732	111	1.985	7.724
	43.260	2.089	4.178	0.0754	200	1.978	7.784
	50.393	1.809	3.618	0.0772	220	1.984	7.731
	74.126	1.277	2.857	0.0787	300	2.207	6.249
Composite	34.951	2.564	4.4442	0.0764	111	1.902	8.414
	43.260	2.089	4.178	0.0788	200	1.892	8.501
	50.393	1.809	3.618	0.0789	220	1.942	8.076
	74.126	1.277	2.857	0.0799	300	2.174	6.441

Table 2: Anti-bacterial parameters

Sample name	Bacteria type	Zone of inhibition
CSN	Cocci	12.5 mm
CSN	Pseudomonas	7.5 mm

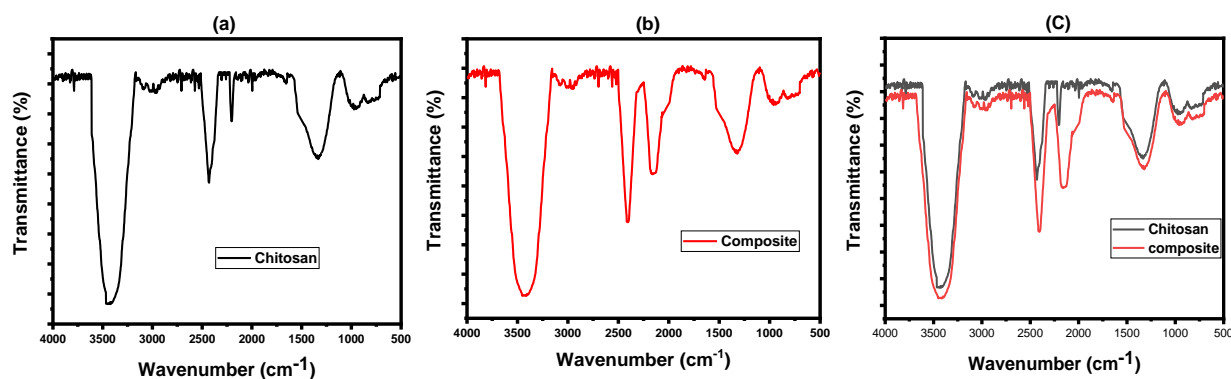


Figure 3: FTIR spectra of (a) pure Chitosan (b) Ag NPs capped with chitosan (c) combined plot.

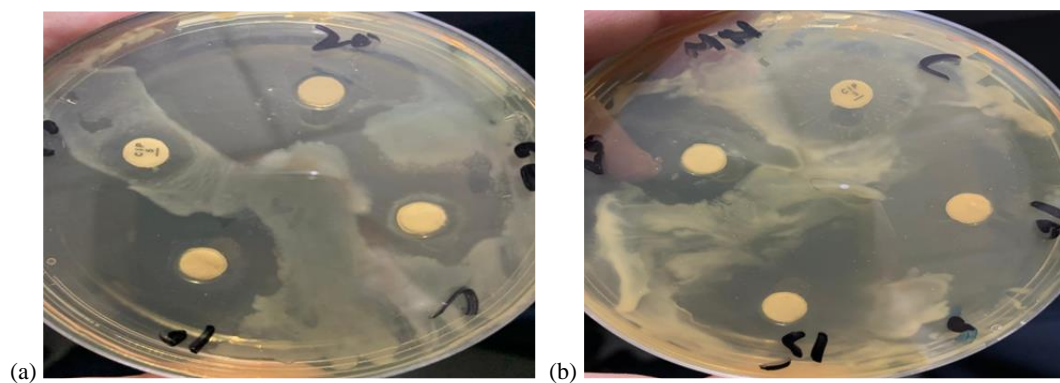


Figure 4: Inhibition zone of Chitosan silver nanocomposite against (a) Cocci bacteria (b) Pseudomonas bacteria

Peaks in the 1000 – 450 cm<sup>-1</sup> range confirm the CH group and –OH out-of-plane deformation of Chi-AgNPs composites. Furthermore, the intensities of amide bands I and III of Chi-Ag-NPs composites at 1644 and 1317 cm<sup>-1</sup> are reduced, it denotes silver nanoparticle chelation with chitosan amino and hydroxyl groups [19].

### 3.4 Antibacterial activity

#### 3.4.1 Calculation of Inhibition zone for gram-positive bacteria cocci

The zone of inhibition was measured using a meter scale or similar physical ruler. The diameter of the petri-dish is measured (in mm) by reading the scale located above it with

the naked eye. We found the inhibition zone by taking different concentration of chitosan nanocomposite that is 10  $\mu\text{L}$ , 15  $\mu\text{L}$ , and 20  $\mu\text{L}$  against gram positive cocci bacteria. It is clear from the results as shown in Figure 4(a) that the inhibition zone generated by composite is much larger as compared to individual components of composite that is silver and chitosan [21]. Moreover, at the concentration of 10 microliter maximum inhibition zone is observed. The inhibition zone for cocci is 1.25 cm or 12.5 mm which is nearest value updated in previous literature.

#### 3.4.2 Calculation of inhibition zone for gram-negative pseudomonas

The zone of inhibition for pseudomonas bacteria which is gram-negative is measured by taking three different concentrations of sample using 10  $\mu\text{L}$ , 15  $\mu\text{L}$ , and 20  $\mu\text{L}$ . It is observed that the zone of inhibition for pseudomonas is 0.75 cm or 7.5 mm, as shown in Figure 4(b). Table 2 contains the summary of these results.

## 4 Conclusions

Chitosan-silver nanocomposite is synthesized using a chemical reduction process and sample exposure to UV light. The targeted composite is made without the use of harmful byproducts and has the maximum effectiveness as an antibacterial, antifungal, and anti-cancerous agent. The addition of chitosan and silver improved the nanocomposite's wound healing and catalytic capabilities. The existence of chitosan silver nanocomposite in the manufactured sample is determined by ultraviolet visible (UV) spectroscopy, with a peak value at 440 nm. Fourier transformation infrared radiation (FTIR) shows the existence of chitosan silver nanocomposites in the product sample's structural and functional groups. The zone of inhibition created by nanocomposites supports their antibacterial efficacy against both gram-positive and gram-negative microorganisms.

### Authors' Credit Statement

**Ansab Ali Zaidi and M. Usman:** Original draft writing, Methodology, Conceptualization, Data curation; **Imosobomeh L. Ikhioya:** Data collection, Reviewing, and Editing; **RY Khosa and A. Atiq:** Supervision, Investigation, and Visualization.

### Declaration of Competing Interest

The authors declare no personal or financial conflicts that may influence the research presented in this paper.

### References

- [1] E. Sánchez-López *et al.*, “Metal-based nanoparticles as antimicrobial agents: An overview,” *Nanomaterials*, vol. 10, no. 2, pp. 1–43, 2020, doi: 10.3390/nano10020292.
- [2] S. Zhang, L. Lin, X. Huang, Y. G. Lu, D. L. Zheng, and Y. Feng, “Antimicrobial Properties of Metal Nanoparticles and Their Oxide Materials and Their Applications in Oral Biology,” *J Nanomater*, vol. 2022, 2022, doi: 10.1155/2022/2063265.
- [3] M. Zhang, W. Xu, M. Li, J. Li, P. Wang, and Z. Wang, “In situ Reduction of Silver Nanoparticles on Chitosan Hybrid Copper Phosphate Nanoflowers for Highly Efficient Plasmonic Solar-driven Interfacial Water Evaporation,” *J Bionic Eng*, vol. 18, no. 1, pp. 30–39, 2021, doi: 10.1007/s42235-021-0005-3.
- [4] I. L. Ikhioya *et al.*, “Enhanced physical properties of nickel telluride metal chalcogenide material with molybdenum dopant,” *Materials Research Innovations*, vol. 00, no. 00, pp. 1–9, 2023, doi: 10.1080/14328917.2023.2222465.
- [5] S. O. Samuel, F. E. James, and I. L. Ikhioya, “Effect of dopant on the energy bandgap on strontium sulphide doped silver for optoelectronic application,” *Materials Research Innovations*, vol. 00, no. 00, pp. 1–11, 2023, doi: 10.1080/14328917.2023.2212944.
- [6] K. Yan, F. Xu, W. Wei, C. Yang, D. Wang, and X. Shi, “Electrochemical synthesis of chitosan/silver nanoparticles multilayer hydrogel coating with pH-dependent controlled release capability and antibacterial property,” *Colloids Surf B Biointerfaces*, vol. 202, no. November 2020, 2021, doi: 10.1016/j.colsurfb.2021.111711.
- [7] D. C. Okeudo *et al.*, “Influence of Polyethylene Glycol (PEG) Surfactant on the Properties of Molybdenum-Doped Zinc Oxide Films,” *Journal of Nano and Materials Science Research*, vol. 2, no. 1, pp. 83–89, 2023.
- [8] N. T. Hiep *et al.*, “Microwave-assisted synthesis of chitosan/polyvinyl alcohol silver nanoparticles gel for wound dressing applications,” *Int J Polym Sci*, vol. 2016, 2016, doi: 10.1155/2016/1584046.
- [9] C. Quintero-Quiroz *et al.*, “Optimization of silver nanoparticle synthesis by chemical reduction and evaluation of its antimicrobial and toxic activity,” *Biomater Res*, vol. 23, no. 1, pp. 1–15, 2019, doi: 10.1186/s40824-019-0173-y.
- [10] E. Susilowati, Maryani, and Ashadi, “Green synthesis of silver-chitosan nanocomposite and their application as antibacterial material,” *J Phys Conf Ser*, vol. 1153, no. 1, 2019, doi: 10.1088/1742-6596/1153/1/012135.
- [11] S. Raza, A. Ansari, N. N. Siddiqui, F. Ibrahim, M. I. Abro, and A. Aman, “Biosynthesis of silver nanoparticles for the fabrication of non cytotoxic and antibacterial metallic polymer based nanocomposite system,” *Sci Rep*, vol. 11, no. 1, pp. 1–15, 2021, doi: 10.1038/s41598-021-90016-w.
- [12] J. Krishna *et al.*, “Synthesis of nanomaterials for biofuel and bioenergy applications,” *Nanomaterials: Application in Biofuels and Bioenergy Production*

- Systems*, pp. 97–165, 2021, doi: 10.1016/B978-0-12-822401-4.00031-3.
- [13] E. Susilowati, Maryani, and Ashadi, “Green synthesis of silver-chitosan nanocomposite and their application as antibacterial material,” in *Journal of Physics: Conference Series*, 2019. doi: 10.1088/1742-6596/1153/1/012135.
- [14] V. Thamilarasan *et al.*, “Single Step Fabrication of Chitosan Nanocrystals Using *Penaeus semisulcatus*: Potential as New Insecticides, Antimicrobials and Plant Growth Promoters,” *J Clust Sci*, vol. 29, no. 2, pp. 375–384, 2018, doi: 10.1007/s10876-018-1342-1.
- [15] S. B. Aziz, O. G. Abdullah, D. R. Saber, M. A. Rasheed, and H. M. Ahmed, “Investigation of metallic silver nanoparticles through UV-Vis and optical micrograph techniques,” *Int J Electrochem Sci*, vol. 12, no. 1, pp. 363–373, 2017, doi: 10.20964/2017.01.22.
- [16] A. Nithya, H. L. Jeevakumari, K. Rokesh, K. Ruckmani, K. Jeganathan, and K. Jothivenkatachalam, “A versatile effect of chitosan-silver nanocomposite for surface plasmonic photocatalytic and antibacterial activity,” *J Photochem Photobiol B*, vol. 153, pp. 412–422, 2015, doi: 10.1016/j.jphotobiol.2015.10.020.
- [17] S. Honary, K. Ghajar, P. Khazaeli, and P. Shalchian, “Preparation, characterization and antibacterial properties of silver-chitosan nanocomposites using different molecular weight grades of chitosan,” *Tropical Journal of Pharmaceutical Research*, vol. 10, no. 1, pp. 69–74, 2011, doi: 10.4314/tjpr.v10i1.66543.
- [18] A. Nithya, H. L. Jeevakumari, K. Rokesh, K. Ruckmani, K. Jeganathan, and K. Jothivenkatachalam, “A versatile effect of chitosan-silver nanocomposite for surface plasmonic photocatalytic and antibacterial activity,” *J Photochem Photobiol B*, vol. 153, pp. 412–422, 2015, doi: 10.1016/j.jphotobiol.2015.10.020.
- [19] P. K. Dara *et al.*, “Synthesis and biochemical characterization of silver nanoparticles grafted chitosan (Chi-Ag-NPs): in vitro studies on antioxidant and antibacterial applications,” *SN Appl Sci*, vol. 2, no. 4, 2020, doi: 10.1007/s42452-020-2261-y.
- [20] J. López-Cuevas, E. Interrial-Orejón, C. A. Gutiérrez-Chavarría, and J. C. Rendón-Ángeles, “Synthesis and Characterization of Cordierite, Mullite and Cordierite-Mullite Ceramic Materials using Coal Fly Ash as Raw Material,” *MRS Adv*, vol. 2, no. 62, pp. 3865–3872, 2017, doi: 10.1557/adv.2018.3.
- [21] P. Sanpui, A. Murugadoss, P. V. D. Prasad, S. S. Ghosh, and A. Chattopadhyay, “The antibacterial properties of a novel chitosan-Ag-nanoparticle composite,” *Int J Food Microbiol*, vol. 124, no. 2, pp. 142–146, 2008, doi: 10.1016/j.ijfoodmicro.2008.03.004.
- [22] Ernest O. Ojegu, Shaka O. Samuel, Mike O. Osiele, Godfrey E. Akpojotor & Imosobomeh L. Ikhioya (2023): Optimisation of deposition voltage of zirconium-doped chromium telluride via typical three-electrode cell electrochemical deposition technique, *Materials Research Innovations*, DOI: 10.1080/14328917.2023.2243063
- [23] Ikhioya, I.L., Nkele, A.C. Properties of electrochemically deposited NiTe films prepared at varying dopant concentrations of molybdenum. *J Mater Sci: Mater Electron* 34, 1603 (2023). <https://doi.org/10.1007/s10854-023-11018-0>
- [24] Shahbaz Afzal, Sidra Tehreem, Tahir Munir, Sakhi G. Sarwar, Imosobomeh L. Ikhioya. Impact of Transition Metal Doped Bismuth Oxide Nanocomposites on the Bandgap Energy for Photoanode Application. *J. Nano & Mat. Sc. Res.* Vol. 2, No. 1 (Maiden edition, 2023), 104 – 109